

## Synthesis and Characterisation of Micronutrient Based Copper Alginate and Ferric Alginate Beads for Agricultural Applications

MOHANAMBAL JOYAL<sup>1,✉</sup>, ANDAL PERUMAL<sup>1,\*✉</sup> and ANBARASU MARIYAPPILLAI<sup>2,✉</sup>

<sup>1</sup>Department of Chemistry, School of Basic Sciences, Vels Institute of Science, Technology and Advanced Studies (VISTAS), Pallavaram, Chennai-600117, India

<sup>2</sup>School of Agriculture, Vels Institute of Science, Technology and Advanced Studies (VISTAS), Pallavaram, Chennai-600117, India

\*Corresponding author: E-mail: andalprithu.sbs@vistas.ac.in

Received: 4 November 2025

Accepted: 30 December 2025

Published online: 6 March 2026

AJC-22283

The excessive use of chemical fertilizers has caused major environmental issues, emphasizing the need for sustainable nutrient delivery systems. In this work, copper and ferric alginate beads were synthesised using the ionotropic gelation method and analysed through UV-DRS, FTIR, FE-SEM, TGA, DSC and AAS techniques. The results showed that  $\text{Cu}^{2+}$  and  $\text{Fe}^{3+}$  ions had been successfully added. The copper beads had porous surfaces and the ferric beads had solid structures. Thermal studies showed that the material was more stable and AAS measured the metal contents at 18.2% Cu and 14.6% Fe. Pot experiments on black gram (*Vigna mungo* L.) showed that ferric alginate beads significant improved plant height (26.5 cm), pod number (32) and seed yield (6.82 g) compared to copper beads. Ferric beads also helped the roots grow better (8.8 cm, 0.75 g dry weight). Based on studies, ferric alginate beads demonstrate strong potential as eco-friendly slow-release fertilizers, while copper alginate beads provide comparatively moderate performance in supporting nutrient release.

**Keywords:** Copper alginate beads, Ferric alginate beads, Micronutrients, Controlled release fertilizer.

### INTRODUCTION

Agriculture stands at the crossroads of producing food for the growing global population and at the same time, maintain the ecological balance. Copper and iron are the two crucial micronutrients for plant growth and metabolic activities. Copper is essential for several enzymatic processes involved in the photosynthesis, respiration and lignin synthesis, and it also plays a defensive role against fungal and bacterial pathogens [1,2]. Similarly, iron is essential for chlorophyll synthesis, electron transport and enzyme activation [3]. However, all these traditional methods of soil/foliar applications of copper and iron salts are inefficient, resulting in leaching, precipitation, low uptake by plants and have low nutrient use efficiency and environmental pollution [4,5]. The overuse of copper-based pesticides, for example, have resulted in large amounts of copper entering to soils and water, causing phytotoxicity, dysfunction of soil microbial ecosystem and long-term ecological risks [6,7]. These issues demand smarter delivery systems for the release in a sustained manner, the minimizing of losses and enhancement of bioavailability [6].

Over the past few years, carriers of biopolymers have received attention as alternative fertilizers [8,9]. Sodium alginate is a naturally occurring polysaccharides extracted from brown seaweeds, which has the advantage of biocompatible, biodegradable and ionotropic gelation [10,11]. Sodium alginate also undergoes the formation of beads containing 3D interconnected microporous structure when crosslinked with bivalent or trivalent ions for the entrapment and release of active substances in a controlled fashion [12,13]. Copper and ferric ions in particular are tightly held to the alginate carboxylate groups which in turn forms highly stable crosslinked networks with a greater structural rigidity [14]. These beads function as micro-reservoirs that release nutrients to the rhizosphere over time, allowing for a more uniform concentration of nutrients over extended periods compared to traditional fertilisation. It has recently been demonstrated that such micro-nutrient-laden alginic acid beads do not only enhance nutrient uptake efficiency, but also decreases leaching losses and with it reduced the risk of groundwater pollution [15].

The importance of copper and ferric alginate beads goes beyond just providing nutrients. Encapsulating copper in algi-

nate has been demonstrated to improve antimicrobial and antifungal effects against common crop pathogens like *Fusarium* species and *Cercospora beticola*. This dual role, serving as both a nutrient provider and a protective agent, makes copper alginate beads especially valuable for sustainable crop management [16]. Ferric-alginate beads have been shown to promote vegetative growth, biomass accumulation and yield with legumes, especially black gram (*Vigna mungo* L.), because iron is required for nodulation and nitrogen fixation [17]. Controlled studies comparing plants treated with ferric-alginate-loaded beads with those treated with copper or left untreated demonstrated that the ferric-alginate-bead-treated plant had greater height, leaf area and dry weight than either untreated or copper-treated plants. This shows that iron plays a bigger role in improving photosynthesis and energy metabolism [18]. Another aspect of these beads is their use in environmental applications. Copper alginate beads are being extensively studied as effective adsorbents for extracting heavy metals and surplus copper from polluted soils and water sources [19,20]. Recently, researchers developed a “remediate-and-sense” system in which alginate-derived beads were used to adsorb copper ions, while electrochemical sensors provided real-time information on the amount of copper being removed. This system was able to achieve over 90% adsorption of copper ions even with very low concentrations of copper in the solution [21]. Furthermore, alginate beads when mixed with ferric ions have been utilised as a magnetic composite for removing contaminants from water. The iron oxide contained within the bead creates a strong enough magnetic attraction to allow easy collection of the alginate beads after they have adsorbed contaminants from the water using magnetic fields [22].

This study employed the ionotropic gelation method to synthesize copper- and ferric-alginate beads, in which sodium ions in sodium alginate were replaced by copper and ferric ions to form stable, cross-linked structures suitable for agricultural applications. The prepared beads were characterized using UV-DRS, FTIR, FE-SEM, TGA, DSC and AAS techniques. Pot-culture experiments using black gram (*Vigna mungo* L.) demonstrated their potential as effective and environmentally friendly carriers for micronutrient delivery in sustainable agriculture.

## EXPERIMENTAL

Copper sulphate pentahydrate ( $\text{CuSO}_4 \cdot 5\text{H}_2\text{O}$ ), iron chloride hexahydrate ( $\text{FeCl}_3 \cdot 6\text{H}_2\text{O}$ ) and sodium alginate, were procured from Sigma-Aldrich, India and used without any additional purification.

**Sodium alginate solution:** For the preparation of sodium alginate solution, 1 g of sodium alginate powder was dissolved in 20 mL of distilled water (at room temperature) by continuous stirring with a magnetic stirrer until completely dissolved, obtaining a homogeneous clear solution. This resulted in a 5.0% (w/v) sodium alginate solution, which was used immediately for the bead preparation.

**Synthesis of alginate beads:** Separate metal salt solution was prepared by dissolving  $\text{CuSO}_4 \cdot 5\text{H}_2\text{O}$  and  $\text{FeCl}_3 \cdot 6\text{H}_2\text{O}$  each in 100 mL of distilled water followed by the addition of

sodium alginate solution was added in a dropwise manner to each metal salt solution, resulting in instantaneous ionotropic gelling and producing spherical beads. The wet beads were then allowed to cure in the metal salt solution for about 10 min to ensure fully crosslinked. Following curing, the wet beads were filtered and rinsed with distilled water to eliminate any excess metal ions were subsequently placed in an oven (50–70 °C) until completely dry.

**Characterisation:** The formation of the alginate beads with copper and ferric ions was confirmed by UV-visible spectrophotometer (Shimadzu UV 5600 plus, Japan) by analysing the absorption bands. The stretching of the M–O bonds and functional groups was analysed using FTIR (Perkin Elmer Spectrum 2, USA). The surface morphology of the alginate beads was observed by FE-SEM (ZEISS SIGMA 300, Germany). Thermal stability and phase transitions were tested by TGA and DSC (TA Instruments, USA) in nitrogen with a heating rate of  $10\text{ }^\circ\text{C min}^{-1}$ . After acid digestion, AAS (Perkin-Elmer PinAAcle 900T, USA) measured the amount of metal (Cu, Fe).

**Pot culture experiment:** Pot culture experiments were taken up in green house to investigate the influence of micronutrient-loaded alginate beads on black gram (*V. mungo* L.). There were treatments of soil application, foliar application and a combination of soil with foliar applications of Cu and Fe alginate beads was placed along with control, in three replications. Clay pots (8 kg capacity) were filled with known soil conditions (consumer available baseline, pH 6.2), adequate moisture and baseline nutrients, followed by sowing of sterilised seeds. Germination was observed a few days after sowing and plants were thinned later to one per pot. The micronutrient beads were manufactured by ionotropic gelation of sodium alginate wherein solution was dripped into  $\text{CuSO}_4$  and  $\text{FeCl}_3$  solutions, followed by curing, washing and drying. Beads were buried 2 to 3 cm below the seeds for soil treatments; foliar treatments were applied at 30 and 45 days after sowing; combination treatments were subjected to a dual application. All pots were watered equally and no other fertilizers were used. Measurements were taken on growth parameters (plant height, number of leaves, leaf size), reproductive characteristics (flowering, pod and seed counts), yield components (weight of 100 seeds, seed yield per plant), biomass (dry matter) and root traits.

## RESULTS AND DISCUSSION

**UV-DRS studies:** Fig. 1a shows the UV-visible spectrum with a distinct absorption peak around 278 nm, attributed to  $\pi \rightarrow \pi^*$  transitions in the alginate polymer backbone. An additional broad absorption band between 450 and 600 nm corresponds to  $d-d$  transitions of  $\text{Cu}^{2+}$  ions, indicating coordination between copper ions and oxygen-containing functional groups in the alginate matrix and confirming successful incorporation of copper into the beads [23]. Similarly, Fig. 1b shows that ferric alginate beads exhibit a strong absorption peak at approximately 230 nm, associated with  $\pi \rightarrow \pi^*$  transitions of alginate. A broad absorption band in the 600–800 nm region is attributed to ligand-to-metal charge-transfer interactions between  $\text{Fe}^{3+}$  ions and alginate functional groups, along with possible

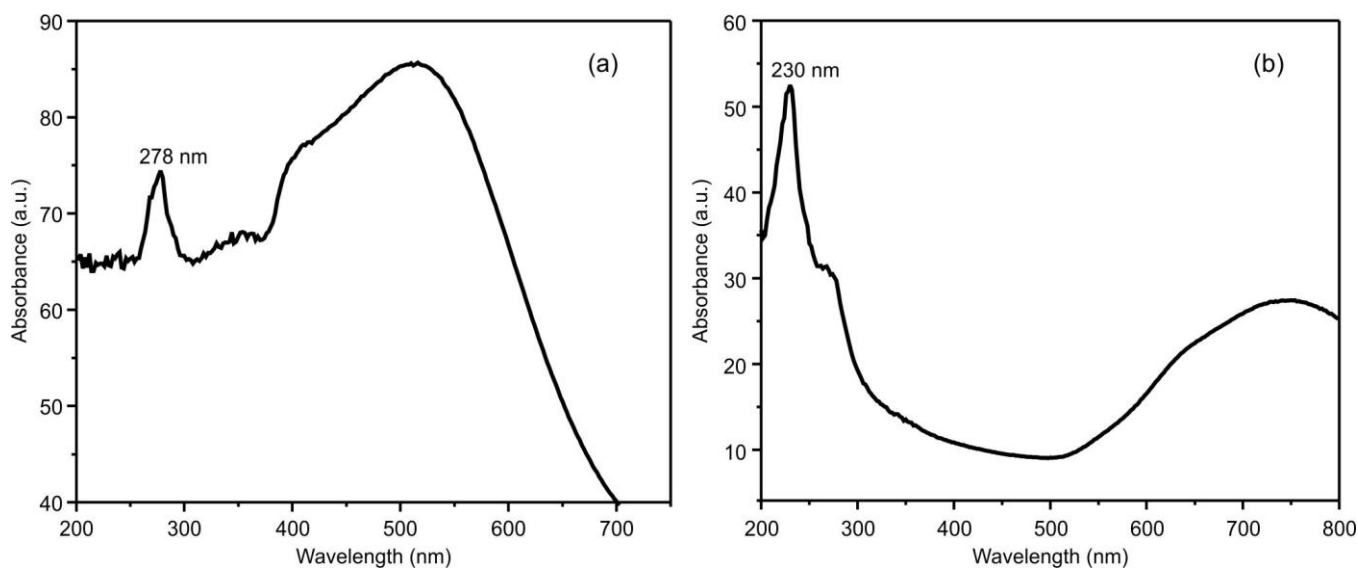


Fig. 1. UV-DRS spectra of (a) copper alginate and (b) ferric alginate beads

*d-d* transitions. These spectral features confirm the coordination and incorporation of ferric ions within the alginate structure [24].

**FTIR studies:** FTIR spectroscopy was conducted to examine the functional groups in copper and ferric alginate beads and to verify their effective interaction between alginate and metal ions. Fig. 2 shows that the spectrum was recorded between 4000 and 400  $\text{cm}^{-1}$ . A wide absorption band found between 3000 and 3600  $\text{cm}^{-1}$  is due to the stretching vibrations of  $-\text{OH}$  groups, which means that alginate has hydroxyl groups. A distinct band observed between 1625 and 1600  $\text{cm}^{-1}$  is attributed to the asymmetric stretching vibration of carboxylate groups, while the peak appearing in the 1450-1410  $\text{cm}^{-1}$  region corresponds to the symmetric stretching vibration of carboxylate groups [25]. Other peaks observed between 1200-1000  $\text{cm}^{-1}$  are linked to the C–O–C and C–O stretching vibrations of the polysaccharide. Peaks appear in the 600-800

$\text{cm}^{-1}$  range are related to M–O interactions, indicating the successful incorporation of  $\text{Cu}^{2+}$  and  $\text{Fe}^{3+}$  ions into the alginate matrix [26,27].

**Morphological studies:** The surface morphology of the prepared copper and ferric alginate beads was analysed using FE-SEM technique. The FE-SEM images of copper alginate beads (Fig. 3a-b) reveal predominantly spherical structures with rough and uneven surfaces. This morphology likely results from the formation of three-dimensional coordination networks between  $\text{Cu}^{2+}$  ions and the carboxylate groups of alginate creating a porous structure that increases surface area. Minor cracking and shrinkage are also observed, possibly due to moisture loss during the drying process [28]. The EDX spectrum of copper alginate beads (Fig. 3c) confirms the presence of Cu (6.97%), O (60.07%), S (9.84%), Na (8.29%), and C (14.83%), verifying successful incorporation of copper ions into the alginate matrix.

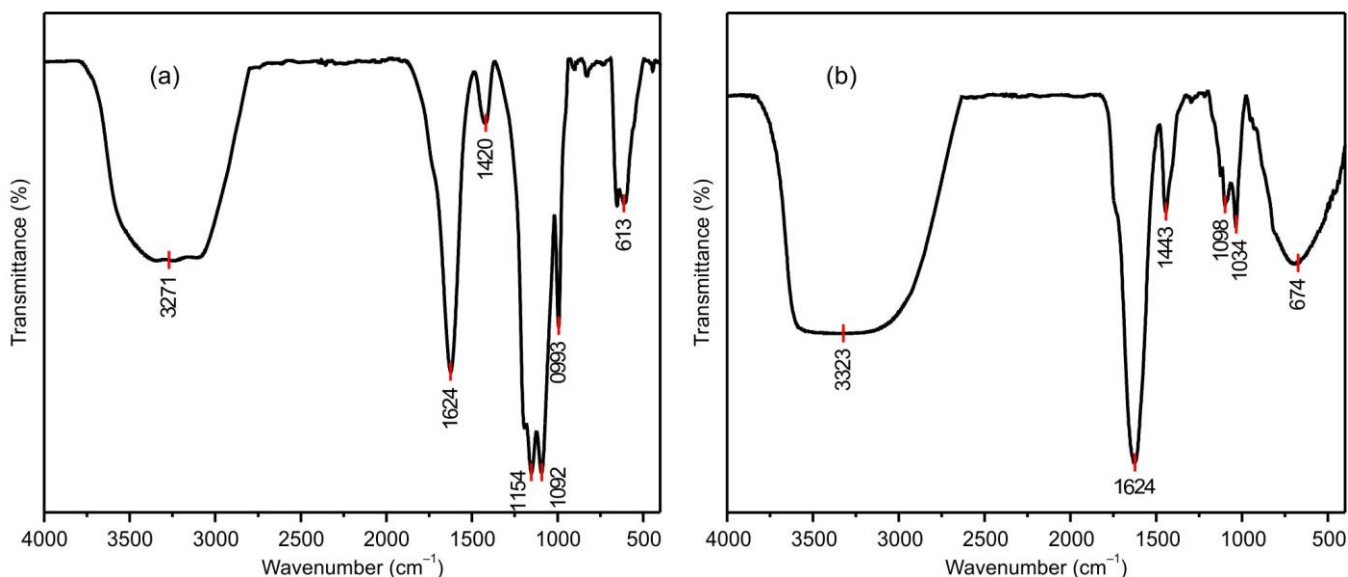


Fig. 2. FTIR spectra of (a) copper alginate and (b) ferric alginate beads

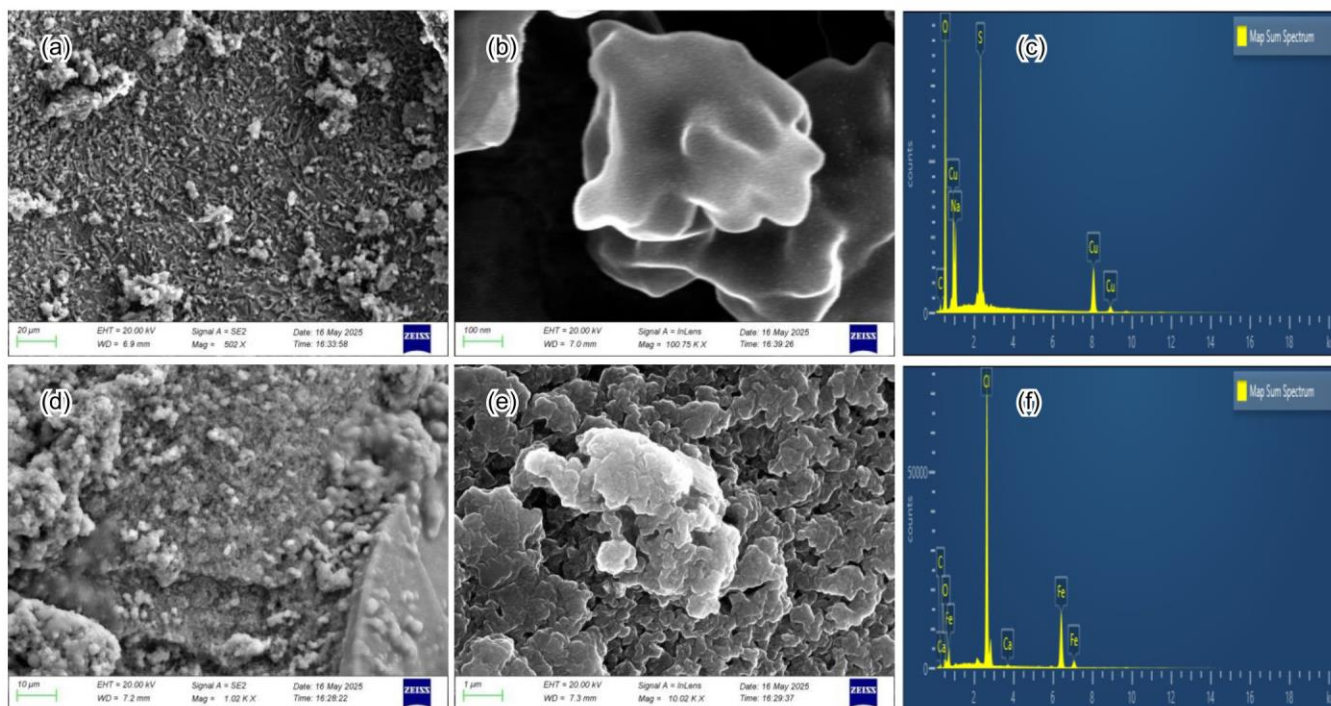


Fig. 3. FE-SEM images of (a,b,c) copper alginate and (d,e,f) ferric alginate beads

Similarly, FE-SEM images of ferric alginate beads (Fig. 3d-e) show nearly spherical particles with a comparatively smoother, denser and more compact surface than copper alginate beads. This morphology suggests stronger crosslinking interactions between  $\text{Fe}^{3+}$  ions and alginate carboxylate groups. Few surface cracks and slight shrinkage are also visible, likely resulting from water evaporation during drying [29]. The EDX analysis of ferric alginate beads (Fig. 3f) indicates the presence of Fe (14.03%), O (21.66%), Ca (0.18%), Cl (28.37%) and C (35.77%). Thus, the morphology result demonstrated that copper and ferric alginate beads were fabricated successfully, exhibiting a high degree of strength as well as the ability to resist deformation. The inclusion of  $\text{Cu}^{2+}$  and  $\text{Fe}^{3+}$  ions

resulted in bead structures with improved integrity and lower porosities.

**Thermal studies:** The TGA curve (Fig. 4a) reveals a multi-step degradation pattern. The initial weight loss below  $150^\circ\text{C}$  is due to the evaporation of physically adsorbed and bound water molecules. A significant weight loss between  $200$  and  $350^\circ\text{C}$  corresponds to the decomposition of the alginate polymer backbone. The breakdown of crosslinked structures and the burning of carbonaceous residues causes the extra weight loss between  $350$  and  $600^\circ\text{C}$ . The weight loss at  $700^\circ\text{C}$ , leaving behind an inorganic residue is due to the formation of stable  $\text{CuO}$ , which confirmed the presence of copper in the alginate matrix. Fig. 4b shows the DSC curve, which sup-

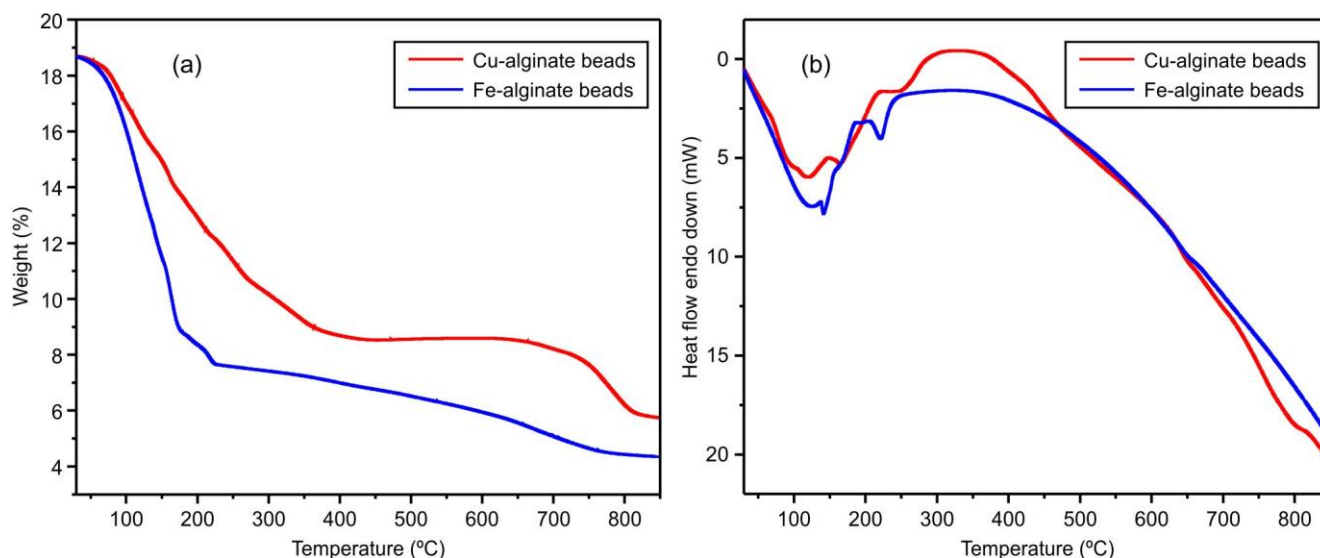


Fig. 4. (a) TGA and (b) DSC curves of copper alginate and ferric alginate beads

orts these thermal changes. An endothermic peak below 150 °C is attributed to dehydration, while the exothermic peaks between 200 and 350 °C correspond to thermal decomposition and oxidation of the alginate matrix. A broad exothermic transition observed above 500 °C is associated with the oxidation of residual carbonaceous material and the stabilization of CuO [30].

The TGA curve of ferric alginate beads shows an initial weight loss below 150 °C, attributed to moisture evaporation, followed by a significant weight reduction between 150 and 300 °C due to decomposition of the alginate backbone. Gradual mass loss continues up to 600 °C, associated with the breakdown of crosslinked structures and combustion of carbonaceous material. Above 700 °C, the mass remains nearly constant, indicating the formation of iron oxide as the final residue. The DSC curve shows an endothermic peak below 150 °C corresponding to the moisture removal, the exothermic peaks between 200 and 350 °C related to polymer decomposition and oxidation, and a broad exothermic transition above 500 °C attributed to oxidation of residual carbon and stabilization of Fe<sub>2</sub>O<sub>3</sub> [31]. These results confirm the successful incorporation of Fe<sup>3+</sup> ions into the alginate matrix and demonstrate the characteristic multistage thermal decomposition behaviour with improved thermal stability compared to pure alginate.

**Environmental analysis:** Atomic absorption spectroscopy (AAS) was used to quantify metal loading in the alginate beads. The results confirm the successful incorporation of metal ions into the alginate matrix. Copper alginate beads contained 18.2% copper, while ferric alginate beads consist of 14.6% iron. The higher copper content suggests stronger interaction or binding affinity of Cu<sup>2+</sup> ions with alginate functional groups compared to Fe<sup>3+</sup> ions, likely due to differences in ionic characteristics and coordination behaviour. These findings demonstrate the effective entrapment of metal ions within the polymer network and indicate the potential of copper and ferric alginate beads as carriers for controlled micronutrient delivery in agricultural applications [32,33].

**Germination and early growth:** The effects of copper and ferric alginate beads on the vegetative growth of black gram (*V. mungo* L.) were evaluated by measuring plant height, leaf length, and leaf width at 20, 40, and 60 days after sowing. The results in Table-1 show that ferric alginate beads helped seeds germinate and plants grow better than copper beads. The mean values clearly show this difference. Plants treated

with F/Fe and SF/Fe reached the greatest heights, averaging 18.4 cm and 17.9 cm. In contrast, the S/Cu and F/Cu treatments produced shorter plants, with mean heights of 11.2 cm and 12.4 cm. A similar trend was observed in leaf size. Ferric treatments produced noticeably longer leaves, measuring 10.9 cm (F/Fe) and 10.8 cm (SF/Fe), compared with 8.5 cm (S/Cu) and 8.8 cm (F/Cu) observed under copper treatments. Leaf width followed the same pattern, with SF/Fe (5.1 cm) and F/Fe (4.6 cm) producing the widest leaves, clearly outperforming the copper treatments. Copper-treated plants, on the other hand, had narrower leaves, with S/Cu (3.2 cm) and F/Cu (3.7 cm) having the narrowest leaves. These mean values confirm that iron plays a more significant role in promoting vegetative vigor through enhanced chlorophyll synthesis, photosynthetic efficiency and enzyme activation, resulting in greater biomass accumulation [34]. In contrast, copper treatments provided only moderate improvements over the control (mean plant height 9.6 cm, leaf length 8.1 cm and leaf width 3.9 cm). In terms of consistent, uniform growth from both a soil application and a foliar application, the use of ferric beads was shown to allow plants to utilize nutrients more efficiently or to have an increased ability to take up nutrients [35]. Although copper treatments did produce some level of increase in growth over that of untreated controls, it was not as clearly defined and did not remain evident in later stages of plant growth. Thus, the superiority of ferric beads in promoting plant growth is due in part to their ability to facilitate processes that are essential for plant growth such as the transport of electrons, respiration and the synthesis of chlorophyll (all processes that require iron) as opposed to processes that require copper alone [36-38].

**Flowering:** Table-2 presents the impact of copper and ferric alginate beads on the time to 50% flowering and the number of flowers per black gram (*V. mungo* L.) plant. The reproductive characteristics of black gram were significantly affected by ferric alginate beads, with plants flowering earlier and producing more flowers than those treated with copper. The average time it took for F/Fe to flower was 35 days, for SF/Fe it was 37 days, for S/Cu it was 39 days and for F/Cu it was 37 days. The experimental plants flowered 50% in an average of 38 days indicated that ferric treatments accelerated the reproductive transition, allowing for earlier flowering than plants treated with copper and untreated plants. The mean number of flowers per plant for the F/Fe and SF/Fe treatments was 25, while the S/Cu and F/Cu treatments produced mean

TABLE-1  
EFFECT OF COPPER AND FERRIC ALGINATE BEADS ON PLANT HEIGHT, LEAF LENGTH AND WIDTH AT 20, 40 AND 60 DAYS OF BLACK GRAM (*Vigna mungo* L.)

Treatment	Plant height (cm)				Leaf length (cm)				Leaf width (cm)			
	20 days	40 days	60 days	Mean value	20 days	40 days	60 days	Mean value	20 days	40 days	60 days	Mean value
S/Fe	10.4	18.7	24.7	17.9	9.0	9.8	9.4	9.4	3.5	5.0	4.5	4.3
S/Cu	6.2	11.2	16.3	11.2	7.4	9.2	8.9	8.5	2.5	3.8	3.5	3.2
SF/Fe	8.6	18.7	26.5	17.9	8.8	12.7	11.1	10.8	4.0	5.4	5.9	5.1
SF/Cu	8.4	15.9	20.4	14.9	8.8	9.1	9.9	9.2	3.5	5	3.3	3.9
F/Fe	11.5	19.2	24.5	18.4	8.4	12.3	12.2	10.9	3.8	5.5	4.6	4.6
F/Cu	5.9	13.2	18.3	12.4	7.5	10.8	8.3	8.8	3.7	4.1	3.5	3.7
Control	5.8	10.9	12.3	9.6	7.4	8.2	8.8	8.1	3.5	5.0	3.3	3.9

TABLE-2  
EFFECT OF COPPER ALGINATE AND FERRIC ALGINATE BEADS ON DAYS TO 50%  
FLOWERING AND NUMBER OF FLOWERS PER PLANT OF BLACK GRAM (*Vigna mungo* L.)

Treatment	50% of flowering (days)				Number of flowers per plant			
	R1	R2	R3	Mean value	R1	R2	R3	Mean value
S/Fe	40	42	43	41	22	35	14	23
S/Cu	37	40	42	39	20	11	13	14
SF/Fe	42	35	36	37	21	24	30	25
SF/Cu	37	36	36	36	28	19	8	18
F/Fe	36	35	35	35	21	24	30	25
F/Cu	37	34	40	37	13	21	17	17
Control	38	38	39	38	19	15	6	13

flower counts of 14 and 17, respectively. The control plants produced the fewest flowers per plant, with an average of 13. Moreover, individual observations showed that SF/Fe plants produced up to 30 flowers, demonstrating the superior influence of ferric beads on flower initiation, abundance and retention. Copper treatments did make more flowers than the control, but they didn't reach the same levels as ferric treatments [39].

**Pod development and yield performance:** Table-3 presents the effects of copper and ferric alginate beads on the number of pods per plant, pod length and seeds per pod of black gram (*V. mungo* L.). The patterns for pod formation and seed formation were the same where ferric bead treatments had more pods and seeds than copper bead treatments. The largest average number of pods per plant occurred with SF/Fe (27), followed by F/Fe (21) during the experimental period. The averages for copper treatments were lower: S/Cu (12) and F/Cu (14) and similar to or just slightly higher than the average for the control (10). The mean pod length was also higher in ferric treatments, with SF/Fe (5.4 cm) and F/Fe (5.3 cm) having the longest pods. In copper treatments, S/Cu (4.7 cm) and F/Cu (4.8 cm) had the shortest pods. This trend also held true for the average number of seeds per pod, which was 7 seeds per pod in F/Fe and S/Fe, 5-6 seeds in copper alginate treatments and only 4 seeds in the control. These findings

validate that ferric alginate beads (SF/Fe and F/Fe) substantially improved the reproductive performance, pod development and seed formation, presumably due to enhanced iron availability that promoted more effective enzyme activation, energy metabolism and nutrient transport during reproductive growth. In contrast, copper beads offered only modest and inconsistent benefits, particularly in pod number and seed formation [40].

Table-3 also illustrates the effects of copper and ferric alginate beads on seed yield per plant and the weight of 100 seeds in black gram. The average seed yield per plant was highest for SF/Fe (5.76 g) and F/Fe (5.55 g), followed closely by S/Fe (4.98 g). On the other hand, copper-based treatments like S/Cu (3.34 g) and F/Cu (2.67 g) produced much lower yields. The control group had the lowest average yield of 2.74 g per plant, which shows that plants don't grow well without extra micronutrients. The mean 100-seed weight was also much higher in plants that had been treated with ferric. The treatments of SF/Fe (5.66 g) and F/Fe (4.91 g) produced the heaviest and most consistent filling of grains, while the average weights produced by the sectors used in the copper treatments were in the range of 4.15-4.27 g, whereas the control had a yield of 4.14 g. Furthermore, this demonstrates that ferric beads are beneficial as they enhance seed numbers, but also

TABLE-3  
EFFECT OF COPPER ALGINATE AND FERRIC ALGINATE BEADS ON NUMBER OF PODS PER PLANT, POD LENGTH,  
SEEDS PER POD, SEED YIELD PER PLANT AND 100 SEEDS WEIGHT OF BLACK GRAM (*Vigna mungo* L.)

Treatment	Pods per plant				Pod length (cm)				Seeds per pod			
	R1	R2	R3	Mean value	R1	R2	R3	Mean value	R1	R2	R3	Mean value
S/Fe	25	18	17	20	5.15	5.38	5.06	5.20	7	7	7	7
S/Cu	24	10	3	12	4.84	4.67	4.60	4.70	5	5	5	5
SF/Fe	32	27	23	27	5.36	5.28	5.56	5.40	6	6	6	6
SF/Cu	24	9	10	14	5.04	4.83	5.13	5.00	6	6	6	6
F/Fe	27	20	16	21	5.24	5.37	5.28	5.30	7	7	7	7
F/Cu	14	16	12	14	4.77	4.70	4.94	4.80	6	6	6	6
Control	10	15	6	10	4.90	4.65	4.55	4.70	4	4	4	4
Treatment	Seed yield per plant (g)				100 seeds weight (g)							
	R1	R2	R3	Mean value	R1	R2	R3	Mean value				
S/Fe	5.38	4.40	5.17	4.98	4.86	4.70	4.75	4.77				
S/Cu	3.14	2.70	4.17	3.34	4.19	4.16	4.09	4.15				
SF/Fe	5.05	6.46	5.78	5.76	5.52	5.77	5.70	5.66				
SF/Cu	2.96	4.91	2.61	3.49	4.27	4.26	4.28	4.27				
F/Fe	4.12	6.82	5.71	5.55	4.87	4.94	4.92	4.91				
F/Cu	2.27	2.99	2.76	2.67	4.15	4.17	4.21	4.18				
Control	2.92	2.75	2.54	2.74	4.10	4.31	4.01	4.14				

in terms of grain filling and size of seed, as well as overall quality, creating a more marketable product. Copper alginate beads showed a slight improvement in yield compared to the control to the control, but their performance was inconsistent, with average yields ranging from 2.67 g to 3.34 g per plant. The continual advantages of ferric beads are due to iron's critical role in the formation of chlorophyll, breathing and moving energy to improve the process of photosynthesis, supporting and concentrating nutrients to help seed production. Copper participates in oxidoreductase systems and redox reactions, but it was not able to produce a reliable yield increase across various replications. The mean values confirm that ferric alginate beads (SF/Fe and F/Fe) provided greater and more reliable productivity in terms of both yield quantity and grain quality, whereas copper beads functioned primarily as supplementary micronutrient sources with limited impact on overall yield outcomes [41,42].

**Root growth and biomass:** Table-4 presents the impact of copper and ferric alginate beads on the root characteristics (length, width and dry weight) and dry matter production of black gram (*V. mungo* L.). Plants treated with ferric and copper alginate beads exhibited distinct differences in roots traits and biomass production. The longest roots were in SF/Fe (8.70 cm) and F/Fe (8.30 cm), followed by S/Fe (8.10 cm). The shortest roots were in copper treatments like S/Cu (7.20 cm) and F/Cu (7.40 cm). The control plants had the shortest mean root length, which was 7.00 cm. Similarly, the mean root width was higher in ferric-treated plants 12.60 cm (SF/Fe) and 12.50 cm (F/Fe) compared to 11.00 cm (S/Cu) and 11.30 cm (F/Cu) among copper-treated plants. The control group had the smallest mean width (8.00 cm) again, which shows that it didn't take in enough nutrients and water. Regarding root dry weight, ferric treatments showed the highest mean values of 0.75 g for both SF/Fe and F/Fe, followed by S/Fe (0.73 g), whereas copper treatments such as S/Cu (0.52 g) and F/Cu (0.54 g) had lighter roots, close to the control (0.51 g). These results clearly suggest that iron supplementation more effectively promotes root elongation, thickness and biomass accumulation than copper treatments, which provided only modest improvements [43,44].

Furthermore, Table-4 also illustrates the effect of copper and ferric alginate beads on the dry matter production (DMP, g/plant) of black gram. The mean DMP was highest in SF/Fe (17.50 g/plant), then in F/Fe (15.05 g/plant) and finally in

S/Fe (13.37 g/plant). The mean DMP was much lower in copper-treated plants (S/Cu (8.25 g/plant) and F/Cu (9.31 g/plant)). The control group had the least amount of biomass, with an average of 7.66 g/plant. These average values show that ferric beads (SF/Fe and F/Fe) were much better than copper beads at improving photosynthetic efficiency, assimilate allocation and total biomass accumulation. Therefore, Iron plays an important role in chlorophyll synthesis, enzyme activation, and electron transport, processes that support carbohydrate production and its translocation to roots and shoots. Copper alginate beads produced a moderate increase in root growth and biomass compared to the control, but the improvements were lower than those observed under ferric treatments in terms of overall growth and productivity. Hence, ferric alginate beads worked much better than copper beads to improve root strength, nutrient uptake and overall plant productivity in black gram [45].

## Conclusion

This study reports the preparation and evaluation of copper and ferric alginate beads as slow-release micronutrient fertilizers for black gram (*V. mungo* L.). Characterization results confirmed the successful incorporation of  $\text{Cu}^{2+}$  and  $\text{Fe}^{3+}$  ions into the alginate matrix. Growth and yield assessments showed that ferric alginate bead treatments (F/Fe and SF/Fe) were more effective than copper alginate beads in promoting both vegetative and reproductive development. Plants treated with ferric beads exhibited greater plant height, larger leaves, higher pod number, increased seed yield and greater dry biomass compared with copper-treated and control plants. The improved performance of ferric beads is attributed to the essential role of iron in chlorophyll formation, enzyme activity, and energy metabolism, which support photosynthesis and nutrient utilization. Copper alginate beads produced moderate improvements in growth, indicating their potential as supplemental micronutrient carriers, although their effectiveness was lower than that of ferric formulations. Thus, the ferric alginate beads were better at encouraging growth and productivity, while copper beads can be used to add nutrients.

## CONFLICT OF INTEREST

The authors declare that there is no conflict of interests regarding the publication of this article.

TABLE-4  
EFFECT OF COPPER ALGINATE AND FERRIC ALGINATE BEADS ON ROOT TRAITS (LENGTH, WIDTH AND DRY WEIGHT) AND DRY MATTER PRODUCTION (DMP, g/plant) OF BLACK GRAM (*Vigna mungo* L.)

Treatment	Root length (cm)				Root width (cm)				Root dry weight (g)				Dey matter production (g/plant)			
	R1	R2	R3	Mean value	R1	R2	R3	Mean value	R1	R2	R3	Mean value	R1	R2	R3	Mean value
S/Fe	7.87	8.16	8.27	8.10	12.41	11.69	11.90	12.00	0.73	0.73	0.73	0.73	13.09	13.28	13.74	13.37
S/Cu	7.48	7.13	6.99	7.20	11.01	10.95	11.04	11.0	0.51	0.51	0.55	0.52	8.41	8.12	8.21	8.25
SF/Fe	8.66	8.87	8.57	8.70	12.32	12.67	12.81	12.60	0.74	0.78	0.73	0.75	17.68	17.46	17.37	17.50
SF/Cu	7.70	7.35	7.45	7.50	12.01	11.37	11.12	11.50	0.56	0.56	0.56	0.56	9.77	9.57	10.26	9.87
F/Fe	8.01	8.20	8.68	8.30	12.82	12.08	12.61	12.50	0.75	0.75	0.75	0.75	14.91	14.64	15.59	15.05
F/Cu	7.28	7.36	7.56	7.40	11.35	11.45	11.10	11.30	0.54	0.53	0.56	0.54	9.63	9.41	8.90	9.31
Control	6.95	6.85	7.20	7.00	8.05	7.79	8.16	8.00	0.52	0.52	0.48	0.51	7.70	7.89	7.38	7.66

## DECLARATION OF AI-ASSISTED TECHNOLOGIES

During the preparation of this manuscript, the authors used an AI-assisted tool(s) to improve the language. The authors reviewed and edited the content and take full responsibility for the published work.

## REFERENCES

1. I. Yruela, *Funct. Plant Biol.*, **32**, 409 (2009); <https://doi.org/10.1071/FP08288>
2. G. Aguirre and M. Pilon, *Front. Plant Sci.*, **6**, 1250 (2016); <https://doi.org/10.3389/fpls.2015.01250>
3. N. Ahmed, B. Zhang, Z. Chachar, J. Li, G. Xiao, Q. Wang, F. Hayat, L. Deng, M.-N. Narejo, B. Bozdar and P. Tu, *Sci. Hortic.*, **323**, 112512 (2024); <https://doi.org/10.1016/j.scienta.2023.112512>
4. J. Niu, C. Liu, M. Huang, K. Liu and D. Yan, *J. Soil Sci. Plant Nutr.*, **21**, 104 (2021); <https://doi.org/10.1007/s42729-020-00346-3>
5. P.S. Bindraban, C. Dimkpa, L. Nagarajan, A. Roy and R. Rabbinge, *Biol. Fertility Soils*, **51**, 897 (2015); <https://doi.org/10.1007/s00374-015-1039-7>
6. M. Fagnano, D. Agrelli, A. Pascale, P. Adamo, N. Fiorentino, C. Rocco, O. Pepe and V. Ventorino, *Sci. Total Environ.*, **734**, 139434 (2020); <https://doi.org/10.1016/j.scitotenv.2020.139434>
7. G. Poggere, A. Gasparin, J.Z. Barbosa, G.W. Melo, R.S. Corrêa and A.C.V. Motta, *J. Trace Elem. Minerals*, **4**, 100059 (2023); <https://doi.org/10.1016/j.jtemin.2023.100059>
8. Q. Chen, M. Gao, Z. Li, Y. Xiao, X. Bai, K.O. Boakye-Yiadom, X. Xu and X.-Q. Zhang, *J. Controlled Rel.*, **323**, 179 (2020); <https://doi.org/10.1016/j.jconrel.2020.03.044>
9. C.S. Reshma, S. Remya and J. Bindu, *Fishery Technol.*, **62**, 16 (2025); <https://doi.org/10.56093/ft.v62i1.153493>
10. A. Sharma and A.K. Singh, *Colloids Interfaces*, **9**, 32 (2025); <https://doi.org/10.3390/colloids9030032>
11. R.S. Alfinaiikh, K.A. Alamry and M.A. Hussein, *RSC Adv.*, **15**, 4708 (2025); <https://doi.org/10.1039/D4RA07277D>
12. Y. Wang, Z. Shen, H. Wang, Z. Song, D. Yu, G. Li, X. Liu and W. Liu, *Gels*, **11**, 16 (2025); <https://doi.org/10.3390/gels11010016>
13. Z. Zou, B. Zhang, X. Nie, Y. Cheng, Z. Hu, M. Liao and S. Li, *RSC Adv.*, **10**, 39722 (2020); <https://doi.org/10.1039/d0ra04316h>
14. Y. Li, Y. Ma, F. Chang, H. Zhu, C. Tian, F. Jia, Y. Ke and J. Dai, *Processes*, **12**, 842 (2024); <https://doi.org/10.3390/pr12040842>
15. K. Yetilmeszoj, E. Kiyani and F. Ilhan, *Int. J. Biol. Macromol.*, **279**, 135382 (2024); <https://doi.org/10.1016/j.ijbiomac.2024.135382>
16. M. Vinceković, S. Jurić, K. Vlahoviček-Kahlina, A. Novak, D. Ivić, L. Hazler, T. Jurkin, A. Bafti and N. Šijaković Vujičić, *Sustainability*, **16**, 5637 (2024); <https://doi.org/10.3390/su16135637>
17. H. Munigala, S. Singh, S.B. Vineetha and B.B. Christina, *J. Exp. Agric. Int.*, **46**, 22 (2024); <https://doi.org/10.9734/jeai/2024/v46i72553>
18. W.I.S.T. Astuti, D.H. Wardhani, Ratnawati, E.A.P.P. Sagala and B.E.I. Siregar, *Food Res.*, **8**, 48 (2024); [https://doi.org/10.26656/fr.2017.8\(S1\).7](https://doi.org/10.26656/fr.2017.8(S1).7)
19. K.Z. Elwakeel, M.M. Ahmed, A. Akhdhar, M.G.M. Sulaiman and Z.A. Khan, *Desalin. Water Treatment*, **272**, 50 (2022); <https://doi.org/10.5004/dwt.2022.28834>
20. Z.A. Sutirman, M.M. Sanagi and W.I.W. Aini, *Int. J. Biol. Macromol.*, **174**, 216 (2021); <https://doi.org/10.1016/j.ijbiomac.2021.01.150>
21. A. Ruccci, M. Metitiero, C. Cuzzi, P.M. Kalligosfyri, M. Messina, M. Spinelli, A. Amoresano, S.L. Woo, I. Cacciotti and S. Cinti, *Analyst*, **149**, 3302 (2024); <https://doi.org/10.1039/D4AN00494A>
22. E. Kalantari, L. Lucia and N. Lavoine, *Green Synth. Catal.*, **3**, 179 (2022); <https://doi.org/10.1016/j.gresc.2022.04.005>
23. D.T.B. Ngoc, D. Bui Duy, L.N.A. Tuan, B.D. Thach, T.P. Tho and D. Van Phu, *Adv. Nat. Sci.: Nanosci. Nanotechnol.*, **12**, 013001 (2021); <https://doi.org/10.1088/2043-6262/abebd6>
24. R.D. Horniblow, M. Dowle, T.H. Iqbal, G.O. Latunde-Dada, R.E. Palmer, Z. Pikramenou and C. Tselepis, *PLoS One*, **10**, e0138240 (2015); <https://doi.org/10.1371/journal.pone.0138240>
25. S.K. Papageorgiou, E.P. Kouvelos, E.P. Favvas, A.A. Sapalidis, G.E. Romanos and F.K. Katsaros, *Carbohydr. Res.*, **345**, 469 (2010); <https://doi.org/10.1016/j.carres.2009.12.010>
26. P. Tordi, F. Ridi, P. Samori and M. Bonini, *Adv. Funct. Mater.*, **35**, 2416390 (2025); <https://doi.org/10.1002/adfm.202416390>
27. Y. Wang, Z. Shen, H. Wang, Z. Song, D. Yu, G. Li, X. Liu and W. Liu, *Gels*, **11**, 16 (2024); <https://doi.org/10.3390/gels11010016>
28. L. Bahsis, E. Ablouh, H. Anane, M. Taourirte, M. Julve and S.-E. Stiriba, *RSC Adv.*, **10**, 32821 (2020); <https://doi.org/10.1039/D0RA06410F>
29. T. Sapkota, S. Shrestha, B.P. Regmi and N. Bhattarai, *RSC Adv.*, **15**, 12876 (2025); <https://doi.org/10.1039/D5RA01397F>
30. M. Elhoudi, R. Oukhrib, C. A. Celaya, D. G. Araiza, Y. Abdellouai, I. Barra, Y. Brahmi, H. Bourzi, M. Reina, A. Albourine and H. Abou Oualid., *J. Mol. Model.*, **28**, 37 (2022); <https://doi.org/10.1007/s00894-022-05028-8>
31. Y. Kabalan, X. Montane, B. Tylkowski, S. De la Flor and M. Giamberini, *Int. J. Biol. Macromol.*, **233**, 123530 (2023); <https://doi.org/10.1016/j.ijbiomac.2023.123530>
32. Y. Moglie, E. Buxaderas, A.G. Cabrera and D.D. Díaz, *Front Chem.*, **13**, 1644592 (2025); <https://doi.org/10.3389/fchem.2025.1644592>
33. O. Churio, F. Pizarro and C. Valenzuela, *Food Hydrocoll.*, **74**, 1 (2018); <https://doi.org/10.1016/j.foodhyd.2017.07.020>
34. T. Tavallali and M.D. Darvishzadeh, *BMC Plant Biol.*, **25**, 905 (2025); <https://doi.org/10.1186/s12870-025-06930-y>
35. G. Chen, J. Li, H. Han, R. Du and X. Wang, *Int. J. Mol. Sci.*, **23**, 12950 (2022); <https://doi.org/10.3390/ijms232112950>
36. A. Sepehri and S. Norimanesh, *Isfahan Univ. Technol.-J. Crop Prod. Process.*, **14**, 47 (2024); <https://doi.org/10.47176/jcpp.14.1.32192>
37. I.F. Carvalho, P.B. Alves, T.C. Ferreira, B.S. Santos, B.B. Cozin, R.P. Souza and L.S. Camargos, *Rev. Caatinga*, **38**, e12686 (2024); <https://doi.org/10.1590/1983-21252025v3812686rc>
38. G.R. Rout and S. Sahoo, *Rev. Agric. Sci.*, **3**, 1 (2015); <https://doi.org/10.7831/ras.3.1>
39. M. Parveen and M. Muthukumar, *Int. J. Ecol. Environ. Sci.*, **49**, 363 (2023); <https://doi.org/10.55863/ije.2023.2663>
40. H. Waheed, M.M. Javaid, A. Shahid, H.H. Ali, J. Nargis and A. Mehmood, *J. Plant Nutr.*, **42**, 1133 (2019); <https://doi.org/10.1080/01904167.2019.1607380>
41. A. Javaid, *Afr. J. Biotechnol.*, **8**, 5189 (2009); <https://doi.org/10.5897/AJB09.793>
42. A.M. Ashraf, H.A. Archana, R. Mahendran, J. Vanitha, S.N. Begam and V. Prakash, *Indian J. Agric. Res.*, **59**, (2025); <https://doi.org/10.18805/IJARE-A-6155>
43. S. Alagarswamy, K.M. Karuppasami, P.B.R. Venugopal, S. Natarajan, M. Djanaguiraman, S. Rathinavelu, V. Dhashnamurthi, R. Veerasamy and B. Parasuraman, *Plants*, **13**, 1549 (2024); <https://doi.org/10.3390/plants13111549>
44. S. Chandwani, A. Gajera, M. Riddhi, H.A. Gamit and N. Amaresan, *J. Appl. Microbiol.*, **134**, lxad189 (2023); <https://doi.org/10.1093/jambio/lxad189>
45. S. Sinha, S. Mondal, S. Maji, P. Dutta and P. Bandopadhyay, *Legume Res.*, **1**, 6 (2022); <https://doi.org/10.18805/LR-4953>